Macromolecules

ARTICLE

pubs.acs.org/Macromolecules

Cross-Linked Nanoporous Materials from Reactive and Multifunctional Block Polymers

Myungeun Seo, Mark A. Amendt, and Marc A. Hillmyer*

Department of Chemistry, University of Minnesota, Minneapolis, Minnesota 55455-0431, United States

Supporting Information

ABSTRACT: Polylactide-*b*-poly(styrene-*co*-2-hydroxyethylmethacrylate) (PLA-*b*-P(S-*co*-HEMA)) and polylactide-*b*-poly(styrene-*co*-2-hydroxyethylacrylate) (PLA-*b*-P(S-*co*-HEA)) were synthesized by combination of ring-opening polymerization and reversible addition−fragmentation chain transfer polymerization. ^{1}H nuclear magnetic resonance spectroscopy and size exclusion chromatography data indicated that the polymerizations were controlled and that hydroxyl groups were successfully incorporated into the block polymers. The polymers were reacted with 4,4′-methylenebis(phenyl isocyanate) (MDI) to form the corresponding cross-linked materials. The materials were annealed at 150 °C to complete the coupling reaction. Robust nanoporous materials were obtained from the cross-linked polymers by treatment with aqueous base to hydrolyze the PLA phase. Small-angle X-ray scattering study combined with scanning electron microscopy showed that MDI-cross-linked PLA-*b*-P(S-*co*-HEMA)/PLA-*b*-P(S-*co*-HEA) can adopt lamellar, hexagonally perforated lamellar, and hexagonally packed cylindrical morphologies after annealing. In particular, the HPL morphology was found to evolve from lamellae due to increase in volume fraction of PS phase as MDI reacted with hydroxyl groups. The reaction also kinetically trapped the morphology by cross-linking. Bicontinuous morphologies were also observed when dibutyltin dilaurate was added to accelerate reaction between the polymer and MDI.

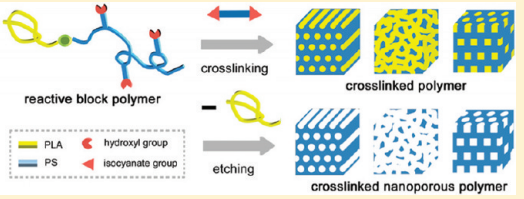

Block copolymers[1] containing an etchable block have been widely explored since well-defined nanoporous materials can be obtained by removal of the sacrificial component from microphase-separated structures.[2] Pore size and morphology are dictated by the molecular weight and composition of the block copolymer. Such nanoporous materials have been demonstrated to be useful as nanofiltration membranes,[3,4] antireflection coatings,[5] and nanotemplates for the synthesis of other nanomaterials.[6] One example of a block that can be readily etched by mild basic hydrolysis is polylactide (PLA).[7] By combining PLA with a variety of other blocks, an assortment of nanoporous structures have been prepared.[7,8]

Although nanoporous materials based on block copolymers offer great chemical tunability, limitations in thermal stability, mechanical performance, and solvent resistance can thwart even broader applications.[8b] Cross-linking has been used to enhance the thermal and chemical stability of block copolymer materials and provides improved mechanical performance. For example, UV irradiation of thin films of the etchable polystyrene-*b*-poly(methyl methacrylate) (PS-*b*-PMMA) has been shown to cross-link polystyrene matrix,[9] and γ-irradiation has been used to cross-link double bonds in the polybutadiene-*b*-poly(methyl methacrylate) (PB-*b*-PMMA) system.[10] Thermal cross-linking has also been demonstrated for PS-based block copolymers containing pendent groups such as benzocyclobutane (BCB)[11] and for PB-[12] or polyisoprene (PI)-based block copolymers[13] with thermal radical initiators. External reagents such as ozone,[14a] S_2Cl_2,[14b] and 1,4-iodobutane[14c] have also been explored for specific cross-linking schemes. In a similar approach, addition polymerization of another monomer in the presence of the block copolymer has been used to form nanostructured thermosets, where one of the blocks contains reactive groups that participate in cross-linking.[8]

Controlled incorporation of highly reactive groups into block copolymers and use of efficient and site-specific cross-linking reactions under mild conditions will expand the utility nanoporous materials. To this end, we have explored the alcohol/isocyanate reaction to form cross-linked block copolymers as precursors to robust nanoporous materials. This reaction has two key advantages: it is highly efficient and it has no side products. Though the feasibility of postmodification[15] and cross-linking[16] of functionalized polymers through reactions with isocyanates for preparation of polymeric nanomaterials has been only recently suggested, the reaction has been utilized in the industrial production of polyurethanes for decades, and a variety of multifunctional alcohols and isocyanates are readily accessible. Also hydroxyl-containing vinyl monomers such as 2-hydroxyethylmethacrylate (HEMA) and 2-hydroxyethylacrylate (HEA) are commercially available and can be incorporated into a polymer backbone through controlled copolymerization strategies.[17,18]

From the view of morphology control, cross-linking kinetically traps the self-assembled structure and can compete with ordering of phase-separated domains. Thus control of the cross-linking

Received: June 20, 2011
Revised: August 25, 2011
Published: November 07, 2011

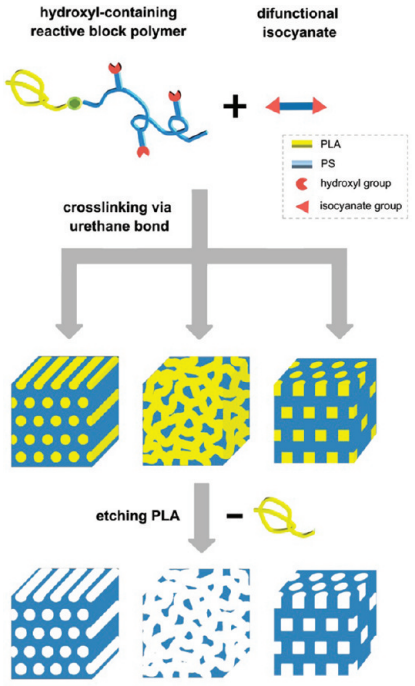

Figure 1. Cross-linked nanoporous polymers by the reaction of hydroxyl-containing block polymers and isocyanates.

rate may also provide a means to obtain varied morphologies from a single precursor.[8] Moreover, metastable phases only observed during phase transitions could possibly be trapped using cross-linking strategies.

Herein we describe the synthesis of hydroxyl-containing reactive block polymers and the formation of urethane cross-linked nanoporous polymers as schematically illustrated in Figure 1. We prepared and utilized reactive block polymers by incorporating hydroxyl groups into the PS block of a PS−PLA block copolymer backbone through a copolymerization scheme. The feasibility of the alcohol−isocyanate reaction for cross-linking of the block copolymer nanostructure was demonstrated by the reaction of the reactive block polymer with 4,4′-methylenebis(phenyl isocyanate) (MDI). Depending on the fraction of PLA and cross-linking reaction rate, different nanostructures were observed. Hydrolysis of the PLA block resulted in cross-linked nanoporous materials that retained the parent morphology.

RESULTS AND DISCUSSION

The synthesis of polylactide-*b*-poly(styrene-*co*-2-hydroxyethylmethacrylate) (PLA-*b*-P(S-*co*-HEMA)) and polylactide-*b*-poly(styrene-*co*-2-hydroxyethylacrylate) (PLA-*b*-P(S-*co*-HEA)) is depicted in Scheme 1. Hydroxyl-terminated PLA was prepared by aluminum catalyzed ring-opening polymerization of D,L-lactide. Then *S*-1-dodecyl-*S*′-(*R*,*R*′-dimethyl-*R*″-acetic acid) trithiocarbonate (CTA),[19] a carboxylic acid-containing chain transfer agent for reversible addition−fragmentation chain transfer (RAFT) polymerization,[18] was coupled with the hydroxyl end via an acid chloride intermediate. The resulting PLA−CTA was characterized by SEC and ^{1}H NMR spectroscopy to confirm complete functionalization (see Figures S1 and S2 in the Supporting Information). This CTA was chosen because it can be readily introduced at the end of the PLA chain and is effective for the

Scheme 1. Synthesis of PLA-*b*-P(S-*co*-HEMA) and PLA-*b*-P(S-*co*-HEA)

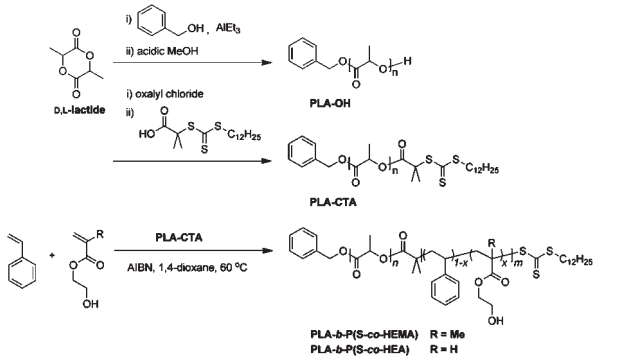

preparation of various PLA-containing block polymers with narrow molecular weight distributions.[20]

Synthesis of PLA-*b*-P(S-*co*-HEMA). SEC analysis of synthesized PLA-*b*-P(S-*co*-HEMA) gave a narrow and unimodal molecular weight distribution and no trace of PLA-CTA (Figure S3a), indicating successful incorporation of PLA-CTA in the RAFT polymerization process. ^{1}H NMR spectra of the polymers were consistent with copolymerization of styrene and HEMA (Figure S3b). From the NMR spectrum, the number-average molecular weight ($M_{n,NMR}$) and the mole fraction of HEMA (x_{HEMA}) were calculated (see Supporting Information). PLA-*b*-P(S-*co*-HEMA) samples with controlled M_n, x_{HEMA}, and narrow molecular weight distributions (PDI values ∼1.2) were obtained.

Reactivity ratios for styrene and HEMA in free radical polymerizations (bulk, 60 °C) have been determined as r_{St} = 0.332 and r_{HEMA} = 0.856.[21] On the basis of this and other RAFT copolymerization studies,[22] we expected HEMA would be selectively incorporated in the earlier stages of the RAFT copolymerization. Indeed, RAFT copolymerization of styrene and HEMA has been reported to produce polymers with higher HEMA incorporation than the feed at low conversion (<25%).[23,24] Starting with 11 mol % HEMA after 43.5 h, the conversion of HEMA (41%) was higher than that of styrene (27%) to yield the x_{HEMA} = 0.17 copolymer with $M_{n,PLA,NMR}$ = 23 kDa and $M_{n,P(S\text{-}co\text{-}HEMA),NMR}$ = 47 kDa (32 wt % of PLA). Copolymerization of styrene and HEMA in the presence of CTA under similar conditions yielded P(S-*co*-HEMA) with 17 mol % of HEMA, suggesting that reactivity ratio of styrene and HEMA was not significantly impacted by the presence of PLA. SEC analysis of this polymer (versus polystyrene standards) gave $M_{n,SEC}$ = 74 kDa and PDI = 1.21. This PLA-*b*-P(S-*co*-HEMA) was used in the following experiments.

Formation of Cross-Linked Nanoporous Polymer. Reaction of PLA-*b*-P(S-*co*-HEMA) with MDI was conducted at room temperature in dry dichloromethane, a good solvent for both blocks. A mixture that was stoichiometrically balanced between isocyanate groups and hydroxyl groups was used (the mass percentage of MDI relative to the block polymer was 12%). A yellow, translucent, and insoluble film was obtained after slow evaporation of solvent overnight at room temperature. The FT-IR spectrum of the film showed a strong absorption at 2268 cm^{-1} (ν_{as}(NCO)) (Figure S4)[25] consistent with unreacted isocyanate. After heating the film to 150 °C for 5 h, we observed a significant reduction in intensity of the ν_{as}(NCO) absorption. Further heating did not lead to significant changes in the IR spectrum. The same

dx.doi.org/10.1021/ma2013942 |*Macromolecules* 2011, 44, 9310–9318

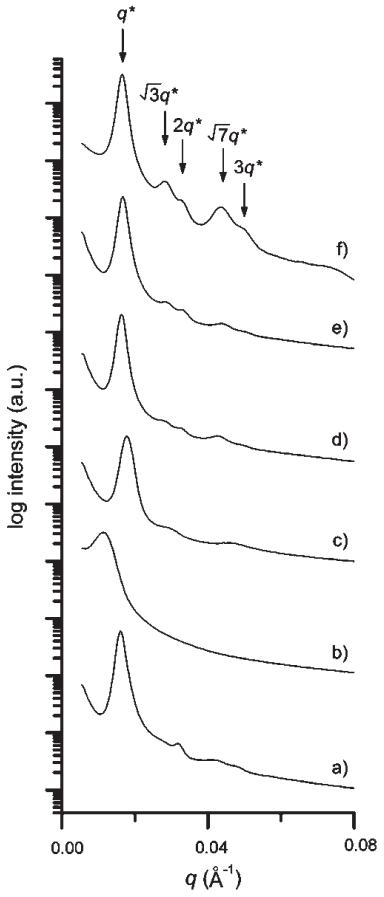

Figure 2. SAXS patterns of polymer films consisting of PLA-*b*-P(S-*co*-HEMA). (a, b) Pure PLA-*b*-P(S-*co*-HEMA) (a) after evaporation of solvent and (b) after annealing at 150 °C. (c) Phenyl isocyanate capped PLA-*b*-P(S-*co*-HEMA) after annealing at 150 °C for 5 h. (d–f) PLA-*b*-P(S-*co*-HEMA) cross-linked with MDI (d) after evaporation of solvent, (e) after annealing at 150 °C for 5 h, and (f) after etching PLA by basic hydrolysis. Arrows show higher-order peak positions that were calculated for hexagonal symmetry based on the primary peak position.

experiment using a thin film cast on a NaCl plate showed 13% of isocyanates reacted after 18 h at room temperature, and the conversion reached 99% after heating at 150 °C for 5 h (Figure S5).

Films of pure PLA-*b*-P(S-*co*-HEMA) after casting from dichloromethane at room temperature gave small-angle X-ray scattering (SAXS) scattering profiles consistent with a hexagonally packed cylindrical morphology with a principal domain spacing of 39 nm (Figure 2a). After annealing of the pure PLA-*b*-P(S-*co*-HEMA) sample at 150 °C for 5 h, the principal peak shifted to a smaller wave vector and broadened to some extent (Figure 2b). The resulting film was insoluble in dichloromethane indicating PLA-*b*-P(S-*co*-HEMA) underwent cross-linking reaction during annealing. We suggest that hydroxyl groups in the PS matrix reacted with the PLA blocks and eventually cross-linked the film by transesterification reactions with PLA.[26] The hydroxyl groups in PLA-*b*-P(S-*co*-HEMA) were end-capped with phenyl isocyanate to form the non-cross-linked analogue and processed following the same protocol as above. After annealing, the hexagonally packed cylindrical morphology of the hydroxyl-end-capped PLA-*b*-P(S-*co*-HEMA) was preserved and the film remained soluble in dichloromethane (Figure 2c). No particular change in the SEC trace before and after annealing was observed in the phenyl isocyanate-capped case.

Differential scanning calorimetry data for the polymers based on PLA-*b*-P(S-*co*-HEMA) was consistent with the SAXS data (Figure S6). When cast from dichloromethane solution, PLA-*b*-P(S-*co*-HEMA) phase separation was indicated by appearance of two T_gs corresponding to PLA (52 °C) and P(S-*co*-HEMA) (92 °C). After annealing at 150 °C for 5 h, T_g of P(S-*co*-HEMA) decreased by 12 °C and the transition enthalpy of PLA significantly decreased. This supports partial mixing of two phases by transesterification of PLA with hydroxyl groups in P(S-*co*-HEMA).[26] When hydroxyl groups of the polymer were end-capped with phenyl isocyanate, both T_gs of PLA and hydroxyl-end-capped P(S-*co*-HEMA) remained unchanged after annealing, supporting that the hydroxyl groups induce transesterification of PLA.

Figure 2d,e show small-angle X-ray scattering (SAXS) scattering patterns of the films of PLA-*b*-P(S-*co*-HEMA) cross-linked with MDI before and after annealing. The film adopted hexagonally packed cylindrical morphology with a domain spacing of 38 nm, which was virtually identical to pure PLA-*b*-P(S-*co*-HEMA); this morphology was unaffected by annealing at 150 °C for 5 h. This is consistent with the preferential reaction of the isocyanate groups in MDI with the hydroxyl groups in the PS block and thus fixing the morphology adopted prior to annealing.

A cross-linked nanoporous polymer was obtained from the MDI cross-linked sample of PLA-*b*-P(S-*co*-HEMA) by mild basic hydrolysis of PLA. The amount of mass loss (29%) was identical to weight fraction of PLA (29%) in the composite sample. FT-IR analysis of the sample post etching showed no trace of ν_{as}(CO) stretching (1755 cm^{-1}) corresponding to PLA (Figure S4).[8b] Stability of the ester and urethane bonds in PS matrix was confirmed by observation of an IR absorption at 1732 cm^{-1} that was attributed to overlapping of ν_{as}(CO) stretching in esters from the HEMA[27] and amide I band in the urethanes.[28] SAXS patterns of the etched sample gave strong scattering intensities due to the increased electron density contrast after removal of PLA and exhibited the same principal spacing and hexagonal symmetry as the precursor (Figure 2f).

Field-emission scanning electron microscope (FE-SEM) images of etched material revealed that hexagonally packed cylindrical pores uniformly span the sample (Figure 3). Cylindrical pores were well organized in each domain and the pore size was uniform all over the material. After accounting for the Pt coating thickness, the pore diameter and center-to-center distances were 25 ± 2 nm and 42 ± 2 nm, respectively. Assuming that density of the cross-linked phase is identical to PS, these values are consistent with values calculated from the SAXS data of 24 and 38 nm, respectively.

Dibutyltin dilaurate (DBTDL) is a well-known catalyst that accelerates alcohol–isocyanate reactions by activation of isocyanates.[29] To test the impact of catalysis, 0.01 and 0.001 equiv of DBTDL relative to hydroxyl groups were added in the PLA-*b*-P(S-*co*-HEMA) + MDI system to accelerate formation of urethane bonds. The influence of the catalyst was determined qualitatively by evaluating the gel time for a solution of PLA-*b*-P(S-*co*-HEMA) and MDI at room temperature. With no catalyst the gel time was estimated to be about 1 day. The same solution with 0.001 equiv of DBTDL became a gel after 20 min, and the solution with 0.01 equiv of DBTDL gelled after 8 min. This indicates that cross-linking occurs much faster when DBTDL is present. The SAXS patterns obtained after consuming all possible isocyanates by drying and annealing at 150 °C for 5 h showed only one broad principal scattering peak for the catalyzed samples (Figure 4b,c), which is consistent with a microphase separated but disorganized structure. Also, the shift of the

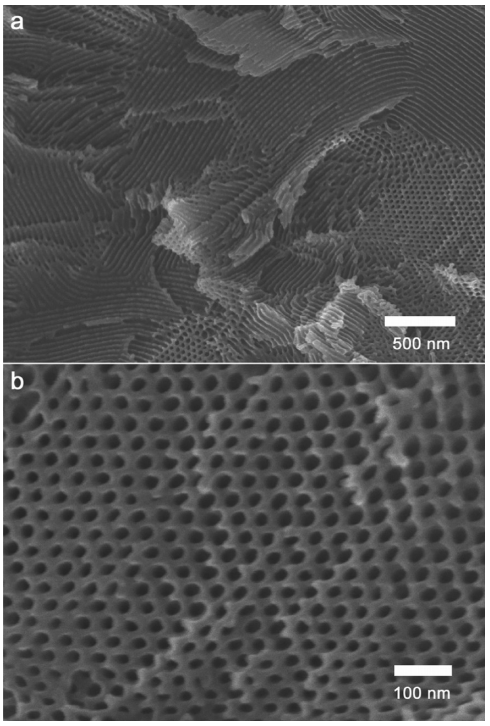

Figure 3. FE-SEM images of cross-linked nanoporous polymer from PLA-*b*-P(S-*co*-HEMA) and MDI showing hexagonally packed cylindrical pores: (a) low magnification; (b) high magnification.

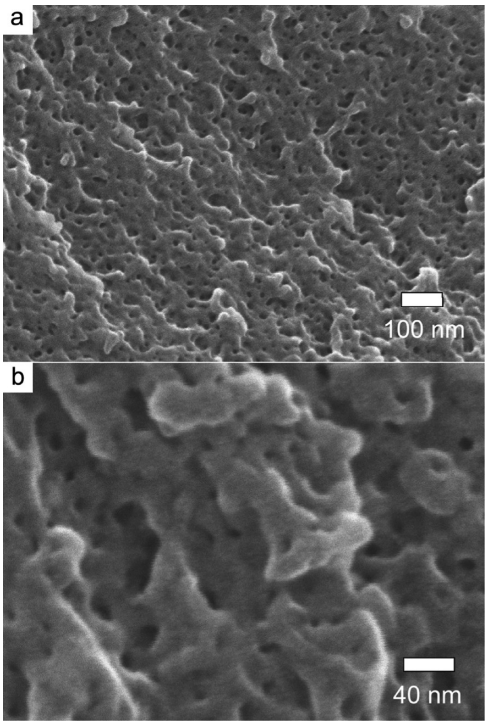

Figure 5. FE-SEM images of cross-linked nanoporous polymer from PLA-*b*-P(S-*co*-HEMA) and MDI in the presence of 0.01 equiv of DBTDL: (a) low magnification; (b) high magnification.

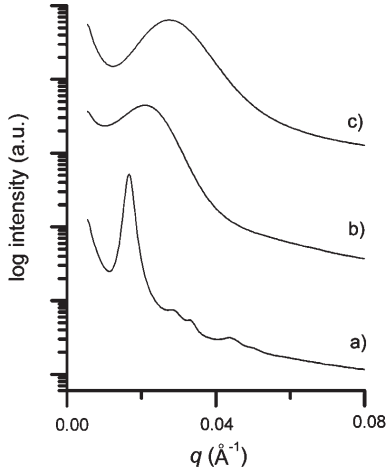

Figure 4. SAXS patterns of (a) PLA-*b*-P(S-*co*-HEMA) cross-linked with MDI after annealing [same data as in Figure 2e], (b) PLA-*b*-P(S-*co*-HEMA) cross-linked with MDI in the presence of 0.001 equiv of DBTDL after annealing at 150 °C for 5 h, and (c) PLA-*b*-P(S-*co*-HEMA) cross-linked with MDI in the presence of 0.01 equiv of DBTDL after annealing at 150 °C for 5 h.

principal peaks toward higher q as compared to the uncatalyzed sample was apparent with increasing concentration of DBTDL. The smaller apparent spacing is likely the result of kinetically trapping a nonequilibrium state, which would restrict mobility of chains and prevent pure domain formation. The exact extent of cross-linking needed for kinetic trapping is not clear at this time.

Etching of the PLA-*b*-P(S-*co*-HEMA) + MDI cross-linked sample prepared using 0.01 equiv of DBTDL showed 27% of mass loss consistent with the PLA content. Figure 5 shows SEM images of the fractured sample revealing holes percolating into the fibrous matrix, supporting formation of bicontinuous porous material. The average diameter of pores was about 15 nm and had a broader distribution compared to cross-linked nanoporous polymer without DBTDL. This is consistent with the broad principal SAXS scattering toward shifted toward higher q (Figure S7c).

However, PLA-*b*-P(S-*co*-HEMA) + MDI cross-linked with 0.001 equiv of DBTDL showed much less mass loss (3%) than weight fraction of PLA (29%) inconsistent with continuous PLA domains. SEM images of the fractured sample also revealed a disordered morphology lacking continuous pores (Figure S8). Unlike our previous work,[8c] the structures formed in this cross-linking strategy are quite sensitive to the cross-linking reaction rate.

DSC thermograms of the cross-linked polymers are shown in Supporting Information (Figure S9). When PLA-*b*-P(S-*co*-HEMA) was cross-linked with MDI, an increase in T_g of P(S-*co*-HEMA) block from 123 to 139 °C was observed after annealing at 150 °C for 5 h. It was attributed to formation of more urethane bonds during annealing producing more branching points and limited segmental motion.[30] After etching, the T_g of PLA was not observed supporting that all the PLA was hydrolyzed, in agreement with FT-IR, SAXS, and weight loss evidence. However, an exothermic transition near temperature of T_g of cross-linked P(S-*co*-HEMA) was observed in the first heating cycle (shown as a dotted line in Figure S9a). This suggests collapse of nanopores as reported previously.[7,8] When 0.01 equiv of DBTDL was added to accelerate the reaction rate, identical trends were observed including an increase in T_g of P(S-*co*-HEMA) block after annealing, disappearance of T_g of PLA after etching, and collapse of nanopores at high temperature. However, when 0.001 equiv of DBTDL was added, the cross-linked polymer showed

Table 1. Composition of PLA-*b*-P(S-*co*-HEMA)s

w_{PLA} (%)	$M_{n,PLA,NMR}$ ($\times10^{-3}$)	$M_{n,P(S\text{-}co\text{-}HEMA),NMR}$ ($\times10^{-3}$)	x_{HEMA} (%)	$M_{n,SEC}$ ($\times10^{-3}$)	PDI
41	20	28	19	50	1.19
39	20	30	18	54	1.18
37	20	33	19	55	1.19
35	20	36	18	57	1.18
33	20	39	18	56	1.21
31	20	42	19	57	1.26

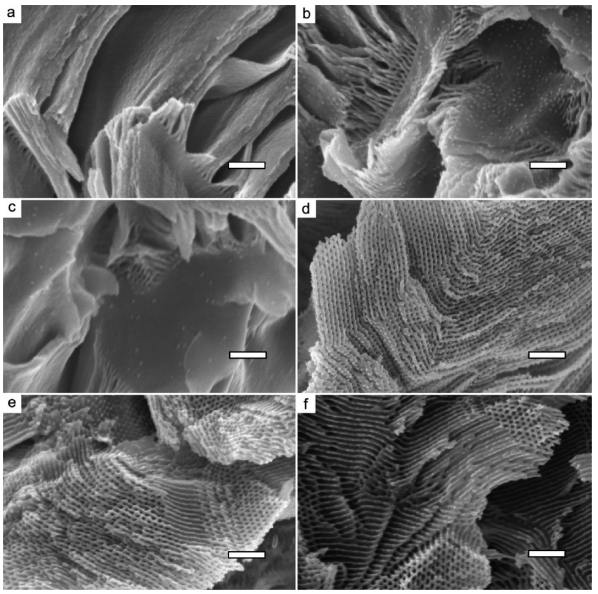

Figure 6. FE-SEM images of cross-linked nanoporous polymers from PLA-*b*-P(S-*co*-HEMA) and MDI with different weight fraction of PLA (w_{PLA}) in the block polymer: (a) 41%, (b) 39%, (c) 37%, (d) 35%, (e) 33%, and (f) 31%. Scale bars represent 100 nm.

only one T_g at 69 °C after annealing at 150 °C (notice there were two T_gs corresponding to PLA and cross-linked P(S-*co*-HEMA) prior to annealing). This suggests a significant degree of mixing between PLA and P(S-*co*-HEMA) similar to that observed in case of annealing pure PLA-*b*-P(S-*co*-HEMA). It seems that a number of unreacted hydroxyl groups were still present prior to annealing when 0.001 equiv of DBTDL was used, and DBTDL preferentially catalyzed transesterification of PLA with the hydroxyl groups over urethane formation at 150 °C, compromising the microphase-separated structure.[31]

PLA-*b*-P(S-*co*-HEMA)s with different weight fractions of PLA (w_{PLA}) were synthesized to access different morphologies. Their compositions are summarized in Table 1 (see Figure S10 for SEC traces). Following the method described above, the polymers were reacted with MDI and annealed at 150 °C for 5 h. Then PLA was etched to form cross-linked nanoporous polymers. The resulting materials were subjected to SEM imaging (Figure 6). When w_{PLA} = 41%, a lamellar morphology was observed that might collapse during etching PLA. Interestingly, at w_{PLA} = 39%, some protruding dots developed on the surface of PS lamellae. These protruded dots were further arranged into hexagonal fashion to form what we tentatively assign to a hexagonally perforated lamellar (HPL) morphology at w_{PLA} = 35%. At w_{PLA} = 33%,

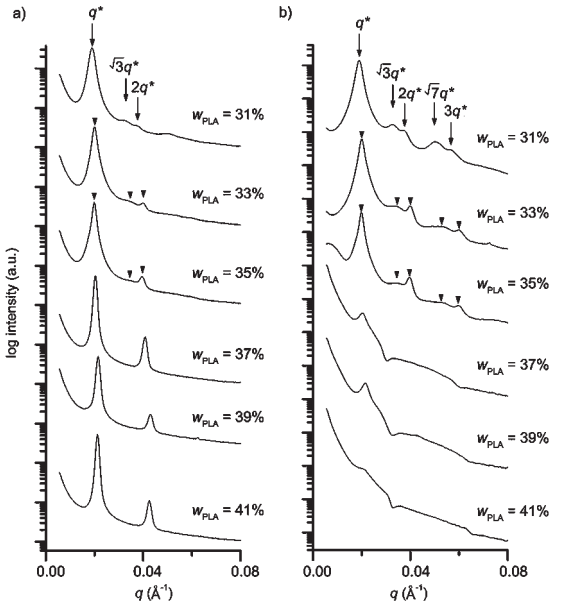

Figure 7. SAXS patterns of PLA-*b*-P(S-*co*-HEMA)s cross-linked with MDI (a) after annealing at 150 °C for 5 h and (b) after etching PLA. Arrows show higher-order peak positions that were calculated for hexagonal symmetry based on the primary peak position.

hexagonally packed cylinders and perforated lamellar morphologies seem to coexist. Only hexagonally packed cylinders appeared with the composition of w_{PLA} = 31%. SAXS patterns of the polymers after annealing and after etching are shown in Figure 7. When w_{PLA} = 41%, lamellae collapsed during etching and the scattering peak was essentially absent after annealing. However, development of HPL morphology stabilized the layers by introducing pillars between them so the scattering patterns were preserved after etching partially when w_{PLA} = 39 and 37%. At w_{PLA} = 35 and 33%, the patterns after annealing could be assigned to a lamellar morphology, but a peak corresponding to $3^{1/2}q^*$ emerged, suggesting development of hexagonal ordering. After etching PLA, the SAXS pattern was more defined and hexagonal ordering was apparent by the presence of broad peaks at $3^{1/2}q^*$ and $7^{1/2}q^*$. Unfortunately, alignment of microdomains could not be performed since the sample was cross-linked. The 2D SAXS patterns were therefore isotropic, and thus definitive assignment of HPL structure based on the scattering was not possible. At w_{PLA} = 31%, the pattern corresponded to hexagonally packed cylinders consistent with SEM data. Interestingly, SAXS patterns of putative HPL structure at w_{PLA} = 35% and the hexagonally packed cylindrical morphology at w_{PLA} = 31% could be distinguished based on the scattering intensity difference between $2q^*$ and $3^{1/2}q^*$, where $2q^*$ was more intense in case of HPL.

The HPL phase assigned to the sample with w_{PLA} = 35% with has been known as a metastable phase observed during the transition between phases.[32−34] A magnified SEM image of the nanoporous cross-linked polymer obtained from PLA-*b*-P(S-*co*-HEMA) with w_{PLA} = 35% confirms HPL morphology revealing staggered stacking of hexagonally perforated PS pillars in successive layers (Figure 8a). Stacking at the domain boundaries is shown in Figure 8b. We speculate that selective incorporation of MDI in PS matrix via the reaction with hydroxyl groups would increase volume fraction of PS and induce phase

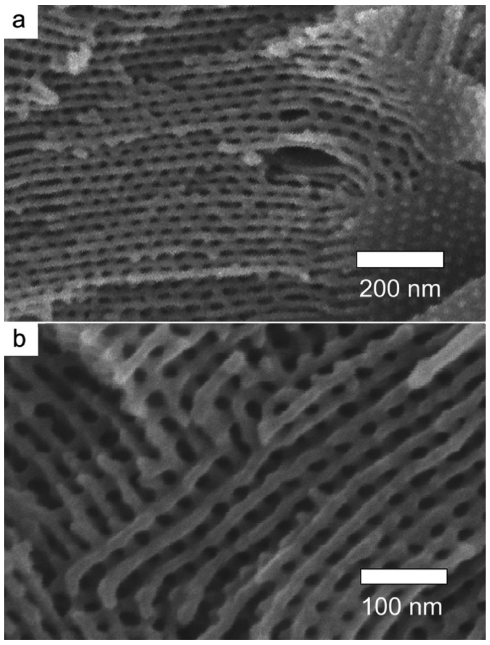

Figure 8. FE-SEM images of cross-linked nanoporous polymers from PLA-*b*-P(S-*co*-HEMA) with w_{PLA} = 35% + MDI.

transition into more PS-rich phases. A similar transition from cylindrical to hexagonal cylinders inside the lamellar morphology by preferential incorporation of cross-linkers in the minority block has been reported.[35]

Time-dependent annealing of PLA-*b*-P(S-*co*-HEMA) with w_{PLA} = 35% + MDI showed that modulation of lamellae began even at room temperature before annealing, evidenced by SEM after etching the polymer (Figure S11a). Well-ordered HPL appeared after 4 h of annealing, but longer annealing did not change the structure presumably due to high degree of cross-linking. This is consistent to the significant consumption of isocyanate after annealing for 4 h indicated by FT-IR (Figure S12). These data suggest initial cross-linking in the lamellae allows modulation only within the lamellar morphology during annealing. Since annealing also accelerates cross-linking reaction, further transition from HPL into more stable phases seems to be prohibited. Time-dependent SAXS patterns also indicated strong development of HPL after annealing for 1 h and not change much afterward (Figure S13).

PLA-*b*-P(S-*co*-HEA). Another PS-*b*-PLA based reactive block polymer, PLA-*b*-P(S-*co*-HEA), was investigated by copolymerization of styrene and 2-hydroxyethyl acrylate. Compared to PLA-*b*-P(S-*co*-HEMA), PLA-*b*-P(S-co-HEA) was expected to possess more homogeneous distribution of hydroxyl groups indicated by close reactivity ratios of styrene and HEA (r_{St} = 0.38, r_{HEA} = 0.34).[36] PLA-*b*-P(S-*co*-HEA) was synthesized following the established condition for PLA-*b*-P(S-*co*-HEMA), and well-defined reactive block polymer with similar compositions was obtained with PDI ∼ 1.2. PLA-*b*-P(S-*co*-HEA)s used for the study are shown in Table 2 (see Figure S14 for SEC and ^{1}H NMR analyses).

Following the fabrication procedure described above, PLA-*b*-P(S-*co*-HEA) was also cross-linked with MDI in dichloromethane solution at room temperature, annealed at 150 °C, and etched in basic solution. SEM images of the polymers confirmed that PLA-*b*-P(S-*co*-HEA) also generated morphologies including lamellae, HPL, and hexagonally packed cylinders according to the weight fraction of PLA, similar to PLA-*b*-P(S-*co*-HEMA) (Figure 9).

Table 2. Composition of PLA-*b*-P(S-*co*-HEA)s

w_{PLA} (%)	$M_{n,PLA,NMR}$ ($\times10^{-3}$)	$M_{n,P(S\text{-}co\text{-}HEA),NMR}$ ($\times10^{-3}$)	x_{HEA} (%)	$M_{n,SEC}$ ($\times10^{-3}$)	PDI
44	23	29	14	62	1.19
38	20	33	12	57	1.22
32	20	41	15	59	1.26

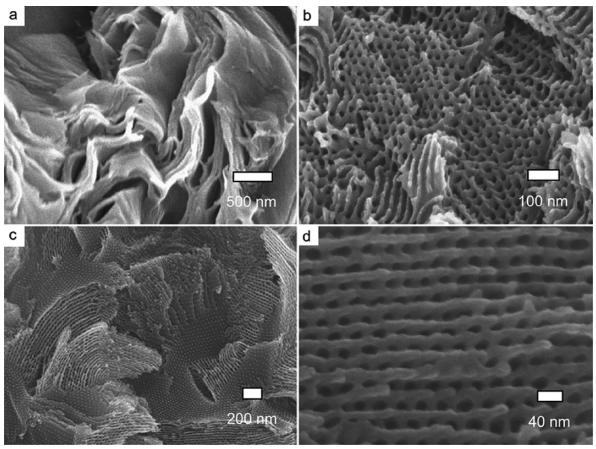

Figure 9. FE-SEM images of cross-linked nanoporous polymers from PLA-*b*-P(S-*co*-HEA) and MDI with different weight fraction of PLA (w_{PLA}) in the block polymer: (a) 44%, (b) 32%, (c) 38%, and (d) magnified image of (c) showing hexagonally perforated lamellar pores.

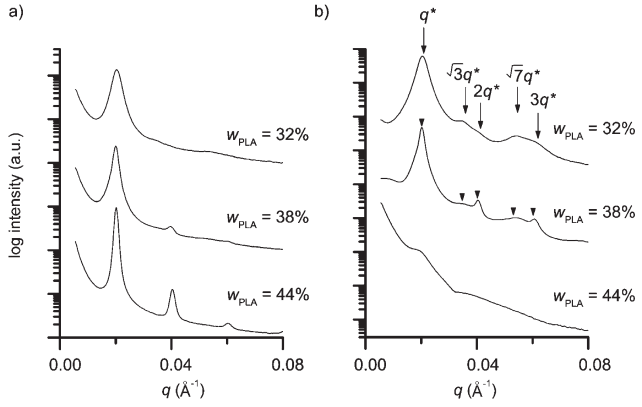

Figure 10. SAXS patterns of PLA-*b*-P(S-*co*-HEA)s cross-linked with MDI (a) after annealing at 150 °C for 5 h and (b) after etching PLA. Arrows show higher-order peak positions that were calculated for hexagonal symmetry based on the primary peak position.

From Figure 9d showing a magnified image of HPL morphology, center-to-center distance of layers was determined to be 33 ± 3 nm and that of cylinders in-plane was 36 ± 2 nm, giving the ratio of 1.1. It is consistent to the previous reports of HPL that have shown relationship between the in-plane spacing (d') and the layer spacing (d^*) is $d' \sim 1.1d^*$.[32b,c,33d,33e,34f] SAXS patterns of the polymers also showed the same trend with PLA-*b*-P(S-*co*-HEMA) and supported the assignment (Figure 10).

It was also possible to obtain bicontinuous porous structure from PLA-*b*-P(S-*co*-HEA) + MDI system by addition of DBTDL. PLA-*b*-P(S-*co*-HEA) with w_{PLA} = 38% was used for the experiment. Appearance of one broad scattering peak and shift toward

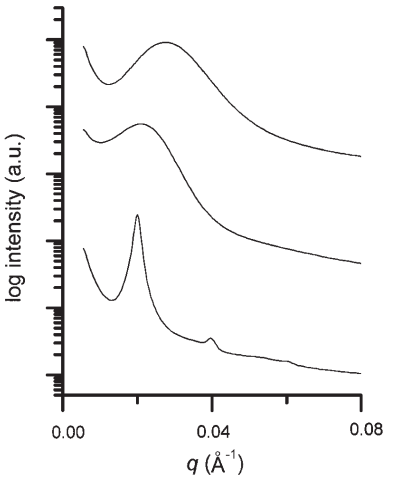

Figure 11. Synchrotron SAXS patterns of (a) PLA-*b*-P(S-*co*-HEA) with w_{PLA} = 38% cross-linked with MDI after annealing [same data as in Figure 10a, middle], (b) PLA-*b*-P(S-*co*-HEA) with w_{PLA} = 38% cross-linked with MDI in the presence of 0.001 equiv of DBTDL after annealing, and (c) PLA-*b*-P(S-*co*-HEA) with w_{PLA} = 38% cross-linked with MDI in the presence of 0.01 equiv of DBTDL after annealing.

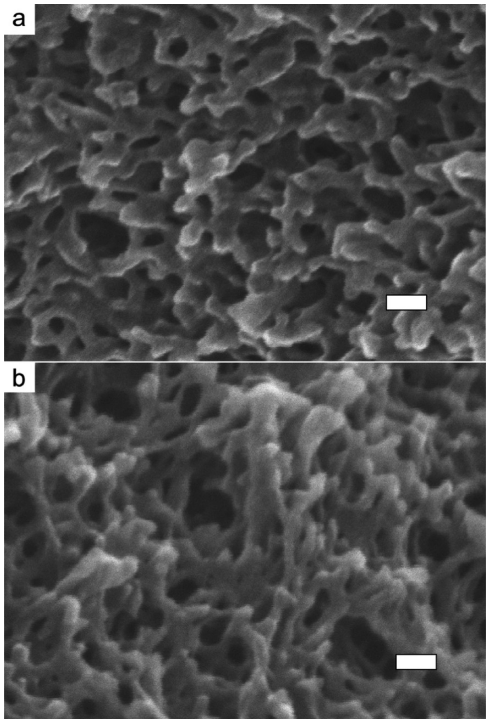

Figure 12. FE-SEM images of cross-linked nanoporous polymer from PLA-*b*-P(S-*co*-HEA) with w_{PLA} = 38% and MDI in the presence of (a) 0.001 equiv of DBTDL and (b) 0.01 equiv of DBTDL. Scale bars represent 40 nm.

high q region upon addition of DBTDL was consistent with PLA-*b*-P(S-*co*-HEMA) case (Figure 11). SEM images of etched samples also confirmed that they possessed bicontinuous porous structure (Figure 12). DSC thermograms of cross-linked polymers showed two T_gs supporting phase separation regardless of the amount of DBTDL. After etching PLA, disappearance of T_g of PLA and exothermic transition corresponding to pore collapse was also observed (Figure S15).

PLA-*b*-P(S-co-HEA) cross-linked with MDI in the presence of DBTDL retained phase separation regardless of the amount of DBTDL, compared to PLA-*b*-P(S-*co*-HEMA) case where the cross-linked film lost phase separation when 0.001 equiv of DBTDL was used. The difference in the distribution of hydroxyl groups between two polymers was attributed to the PLA-*b*-P(S-*co*-HEA) having more homogeneously distributed hydroxyl groups and more chances to cross-link in the PS domain rather than to transesterify PLA.

CONCLUSION

Controlled synthesis of two hydroxyl-containing reactive block polymers PLA-*b*-P(S-*co*-HEMA) and PLA-*b*-P(S-*co*-HEA) was achieved by combination of ring-opening polymerization and RAFT polymerization. When the polymer was cross-linked with MDI through urethane bond formation and PLA was etched out, well-defined cross-linked nanoporous polymers with different morphologies including lamellae, hexagonally packed cylinders, and HPL were obtained. The HPL morphology was obtained by increase in volume fraction of PS phase as MDI reacted with hydroxyl groups, and it was stable because of cross-linking. This demonstrates possibility of morphology control/locking by cross-linking. Also, it was possible to obtain bicontinuous morphology by tuning the reaction rate by use of DBTDL. The successful use of urethane bonds for cross-linked nanoporous materials suggests that the class of materials that can be made is significantly expanded by employing other types of reactions used for synthesis of step-growth polymers such as polyamides and polyesters.

EXPERIMENTAL DETAILS

Materials. Unless specifically noted, all chemicals were purchased from Sigma-Aldrich (St. Louis, MO). Benzyl alcohol (anhydrous, 99.8%), triethylaluminum solution (1.0 M in hexanes), 1,4-dioxane (anhydrous, 99.8%), phenyl isocyanate (≥98%), 4,4′-methylenebis(phenyl isocyanate) (MDI) (98%), and dibutyltin dilaurate (DBTDL) (95%) were used without further purification. Azobisisobutyronitrile (AIBN) (98%) was recrystallized from methanol and dried *in vacuo* overnight. Styrene (≥99%) and 2-hydroxyethyl methacrylate (HEMA) (97%) were passed through a basic alumina column prior to use. 2-Hydroxyethyl acrylate (HEA) (≥97%) was purchased from Fluka and passed through a basic alumina column. D,L-Lactide (99%) purchased from Purac was recrystallized from toluene and stored under a N_2 atmosphere. All bulk solvents were purchased from Mallinckrodt (Hazelwood, MO) and used as received unless otherwise specified. Dichloromethane (HPLC grade) was purified on an MBraun solvent purification system. *S*-1-Dodecyl-*S*′-(*R*,*R*′-dimethyl-*R*″-acetic acid) trithiocarbonate (CTA) was prepared using a reported procedure.[19] Hydroxyl-terminated polylactide (PLA-OH) and trithiocarbonate end-capped PLA (PLA-CTA) were prepared by following procedures reported elsewhere.[20]

Characterization. ^{1}H nuclear magnetic resonance (NMR) spectroscopy was conducted using a Varian Inova 500 MHz instrument spectrometer with the residual solvent signal as an internal reference. Size exclusion chromatography (SEC) was performed in chloroform at 35 °C on a Hewlett-Packard 1100 series liquid chromatograph (Palo Alto, CA) equipped with three PLgel 5 μm Mixed-C columns in series with molecular weight range 400−400 000 g mol^{-1}. A Hewlett-Packard 1047A refractive index detector was employed. The molecular

weights of the polymers were calculated relative to linear polystyrene standards from Varian, Inc. (Palo Alto, CA). Fourier transform infrared (FT-IR) spectra were obtained on a Nicolet Magna-IR spectrometer 550 using the KBr pellet technique or a thin film cast on a NaCl plate. Synchrotron small-angle X-ray scattering (SAXS) experiments were performed at the Advanced Photon Source (APS) at Argonne National Laboratories at Sector 5-ID-D beamline. The beamline is maintained by the Dow−Northwestern−Dupont Collaborative Access Team (DND-CAT). The source produces X-rays with a wavelength of 0.84 Å. Scattering intensity was monitored by a Mar 165 mm diameter CCD detector with a resolution of 2048 × 2048. The two-dimensional scattering patterns were azimuthally integrated to afford one-dimensional profiles presented as spatial frequency (q) versus scattered intensity. Scanning electron microscope (SEM) images were obtained on a Hitachi S-4900 FE-SEM instrument using a 3−5 kV accelerating voltage. Prior to SEM analysis, cryo-fractured monoliths were coated with a ca. 1 nm thick platinum layer via direct platinum sputtering using a VCR ion beam sputter coater. Differential scanning calorimetry (DSC) study was conducted on a TA Q1000 instrument using a scan rate of 10 °C/min under an inert atmosphere.

Synthesis of PLA-*b*-P(S-*co*-HEMA)/PLA-*b*-P(S-*co*-HEA). Synthesis of PLA-*b*-P(S-*co*-HEMA) is illustrated. PLA-CTA (0.573 g, 24.9 μmol), styrene (3.555 g, 34.1 mmol), HEMA (0.528 g, 4.06 mmol), AIBN (0.059 g, 3.91 μmol (as a 1.1 wt % benzene solution)), and 1,4-dioxane (0.6 mL) were placed in a Schlenk flask. The flask was degassed by three freeze−pump−thaw cycles and placed in a preset oil bath at 60 °C for 43.5 h. After cooling to room temperature, the solution was diluted with dichloromethane and precipitated into methanol (ca. 400 mL). The precipitate was filtered and dried *in vacuo* to give the desired copolymer (1.448 g, 31%). M_n (NMR) 7.02 × 10^4. M_n (SEC) 7.35 × 10^4. Polydispersity index (PDI): 1.21.

PLA-*b*-P(S-*co*-HEA)s were synthesized using the same condition described above using HEA instead of HEMA.

End-Capping Hydroxyl Groups with Phenyl Isocyanate. PLA-*b*-P(S-*co*-HEMA) or PLA-*b*-P(S-*co*-HEA) (0.2 g) was dissolved in dry dichloromethane (10 mL), and DBTDL (0.05 equiv relative to hydroxyl groups, 1% v/v solution in dichloromethane) was added and stirred. To the solution, phenyl isocyanate (5 equiv relative to hydroxyl groups, 4% v/v solution in dichloromethane) was added and stirred at room temperature overnight. The reaction mixture was filtered and precipitated into methanol (ca. 100 mL) to produce end-capped polymer with quantitative yield. ^{1}H NMR spectra of the hydroxyl-end-capped polymers in DMSO-d_6 showed additional peaks at 9.7 and 7.5 ppm which correspond to carbamate and phenyl protons, confirming that phenyl carbamate had formed.

General Procedure for Fabrication of Cross-Linked Nanoporous Polymer. PLA-*b*-P(S-*co*-HEMA) or PLA-*b*-P(S-*co*-HEA) (0.2 g) was dissolved in dichloromethane (1 mL) and transferred into a polypropylene vial. 4,4-Methylenebis(phenyl isocyanate) (0.5 equiv relative to hydroxyl groups, 20 wt % solution in dichloromethane) was added into the vial and thoroughly mixed. The solution was allowed to evaporate under a N_2 atmosphere overnight. The resulting film was dried in a vacuum oven, annealed at 150 °C for 5 h, and etched in 0.5 M NaOH solution (H_2O/methanol = 6/4) at 70 °C for 3 days. Etched pieces were thoroughly washed with deionized water and methanol and dried under N_2 purging. In case of using DBTDL to accelerate reaction, DBTDL solution in dichloromethane was added prior to add MDI. Using the same protocol, films of PLA-*b*-P(S-*co*-HEMA), PLA-*b*-P(S-*co*-HEA), and hydroxyl-end-capped polymers were fabricated without addition of MDI.

■ ASSOCIATED CONTENT

Ⓢ Supporting Information. Figures S1−S15. This material is available free of charge via the Internet at http://pubs.acs.org.

■ AUTHOR INFORMATION

Corresponding Author
*E-mail: hillmyer@umn.edu.

■ ACKNOWLEDGMENT

We thank Dow Chemical Company for financial support. This work was also partially funded by the National Science Foundation (DMR 1006370). Parts of this work were carried out in the Institute of Technology Characterization Facility, University of Minnesota, a member of the NSF-funded Materials Research Facilities Network. SAXS data were acquired at the DuPont-Northwestern-Dow Collaborative Access Team (DND-CAT) located at Sector 5 of the Advanced Photon Source (APS). DND-CAT is supported by E.I. DuPont de Nemours & Co., The Dow Chemical Company and Northwestern University. Use of the APS, an Office of Science User Facility operated for the U.S. Department of Energy (DOE) Office of Science by Argonne National Laboratory, was supported by the U.S. DOE under Contract No. DE-AC02-06CH11357.

■ REFERENCES

(1) Hadjichristidis, N.; Pispas, S.; Floudas, G. A. *Block Copolymers: Synthetic Strategies, Physical Properties, and Applications*; Wiley-Interscience: New York, 2003.

(2) (a) Hamley, I. W. *Nanotechnology* **2003**, *14*, R39–R54. (b) Olson, D. A.; Chen, L.; Hillmyer, M. A. *Chem. Mater.* **2008**, *20*, 869–890.

(3) (a) Phillip, W. A.; Rzayev, J.; Hillmyer, M. A.; Cussler, E. L. *J. Membr. Sci.* **2006**, *286*, 144–152. (b) Philip, W. A.; O'Neill, B.; Rodwogin, M.; Hillmyer, M. A.; Cussler, E. L. *ACS Appl. Mater. Interfaces* **2010**, *2*, 847–853. (c) Jackson, E. A.; Hillmyer, M. A. *ACS Nano* **2010**, *4*, 3548.

(4) (a) Yang, S. Y.; Ryu, I.; Kim, H. Y.; Kim, J. K.; Jang, S. K.; Russell, T. P. *Adv. Mater.* **2006**, *18*, 709–712. (b) Yang, S. Y.; Park, J.; Yoon, J.; Ree, M.; Jang, S. K.; Kim, J. K. *Adv. Funct. Mater.* **2008**, *18*, 1371–1377.

(5) (a) Walheim, S.; Schaffer, E.; Mlynek, J.; Steiner, U. *Science* **1999**, *283*, 520–522. (b) Joo, W.; Park, M. S.; Kim, J. K. *Langmuir* **2006**, *22*, 7960–7963. (c) Joo, W.; Kim, H. J.; Kim, J. K. *Langmuir* **2010**, *26*, 5110–5114.

(6) (a) Thurn-Albrecht, T.; Schotter, J.; Kastle, G. A.; Emley, N.; Shibauchi, T.; Krusin-Elbaum, L.; Guarini, K.; Black, C. T.; Tuominen, M. T.; Russell, T. P. *Science* **2000**, *290*, 2126–2129. (b) Crossland, E. J. W.; Ludwigs, S.; Hillmyer, M. A.; Steiner, U. *Soft Matter* **2007**, *3*, 94–98. (c) Crossland, E. J. W.; Nedelcu, M.; Ducati, C.; Ludwigs, S.; Hillmyer, M. A.; Steiner, U.; Snaith, H. J. *Nano Lett.* **2009**, *9*, 2813–2819.

(7) (a) Zalusky, A. S.; Olayo-Valles, R.; Taylor, C. J.; Hillmyer, M. A. *J. Am. Chem. Soc.* **2001**, *123*, 1519–1520. (b) Zalusky, A. S.; Olayo-Valles, R.; Wolf, J. H.; Hillmyer, M. A. *J. Am. Chem. Soc.* **2002**, *124*, 12761–12773.

(8) (a) Chen, L.; Phillip, W. A.; Cussler, E. L.; Hillmyer, M. A. *J. Am. Chem. Soc.* **2007**, *129*, 13786–13787. (b) Chen, L.; Hillmyer, M. A. *Macromolecules* **2009**, *42*, 4237–4243. (c) Amendt, M. A.; Chen, L.; Hillmyer, M. A. *Macromolecules* **2010**, *43*, 3924–3934.

(9) Misner, M. J.; Skaff, H.; Emrick, T.; Russell, T. P. *Adv. Mater.* **2003**, *15*, 221–224.

(10) Sekine, R.; Sato, N.; Matsuyama, T.; Akasaka, S.; Hasegawa, H. *J. Polym. Sci., Part A: Polym. Chem.* **2007**, *45*, 5916–5922.

(11) Leiston-Belanger, J. M.; Russell, T. P.; Drockenmuller, E.; Hawker, C. J. *Macromolecules* **2005**, *38*, 7676–7683.

(12) Guo, F.; Andreasen, J. W.; Vigild, M. E.; Ndoni, S. *Macromolecules* **2007**, *40*, 3669–3675.

(13) (a) Cavicchi, K. A.; Zalusky, A. S.; Hillmyer, M. A.; Lodge, T. P. *Macromol. Rapid Commun.* **2004**, *25*, 704–709. (b) Hansen, M. S.; Vigild, M. E.; Berg, R. H.; Ndoni, S. *Polym. Bull.* **2004**, *51*, 403–409.

(14) (a) Jeong, U.; Ryu, D. Y.; Kim, J. K.; Kim, D. H.; Wu, X.; Russell, T. P. *Macromolecules* **2003**, *36*, 10126–10129. (b) Zhou, N.; Bates, F. S.;

Lodge, T. P. *Nano Lett.* **2006**, *6*, 2354–2357. (c) Okumura, A.; Nishikawa, Y.; Hashimoto, T. *Polymer* **2006**, *47*, 7805–7812.

(15) Biedermann, F.; Appel, E. A.; del Barrio, J.; Gruendling, T.; Barner-Kowollik, C.; Scherman, O. A. *Macromolecules* **2011**, *44*, 4828–4835.

(16) Beck, J. B.; Killops, K. L.; Kang, T.; Sivanandan, K.; Bayles, A.; Mackay, M. E.; Wooley, K. L.; Hawker, C. J. *Macromolecules* **2009**, *42*, 5629–5635.

(17) (a) Matyjaszewski, K.; Davis, T. P. *Handbook of Radical Polymerization*; John Wiley and Sons, Inc.: New York, 2002. (b) Matyjaszewski, K.; Xia, J. *Chem. Rev.* **2001**, *101*, 2921–2990. (c) Hawker, C. J.; Bosman, A. W.; Harth, E. *Chem. Rev.* **2001**, *101*, 3661–3688.

(18) (a) Moad, G.; Rizzardo, E.; Thang, S. H. *Acc. Chem. Res.* **2008**, *41*, 1133–1142. (b) Moad, G.; Rizzardo, E.; Thang, S. H. *Aust. J. Chem.* **2006**, *59*, 669–692. (c) Moad, G.; Rizzardo, E.; Thang, S. H. *Aust. J. Chem.* **2009**, *62*, 1402–1472. (d) Monteiro, M. J. *J. Polym. Sci., Part A: Polym. Chem.* **2005**, *43*, 3189–3204. (e) Barner, L.; Davis, T. P.; Stenzel, M. H.; Barner-Kowollik, C. *Macromol. Rapid Commun.* **2007**, *28*, 539–559.

(19) Lai, J. T.; Filla, D.; Shea, R. *Macromolecules* **2002**, *35*, 6754–6756.

(20) Rzayev, J.; Hillmyer, M. A. *J. Am. Chem. Soc.* **2005**, *127*, 13373–13379.

(21) (a) Greenley, R. Z. *J. Macromol. Sci., Chem.* **1980**, *14*, 427. (b) Galbraith, M. N.; Moad, G.; Solomon, D. H.; Spurling, T. H. *Macromolecules* **1987**, *20*, 675–679. (c) Liang, K.; Dossi, M.; Moscatelli, D.; Hutchinson, R. A. *Macromolecules* **2009**, *42*, 7736–7744.

(22) Feldermann, A.; Toy, A. A.; Phan, H.; Stenzel, M. H.; Davis, T. P.; Barner-Kowollik, C. *Polymer* **2004**, *45*, 3997–4007.

(23) (a) Xu, X.; Huang, J. *J. Polym. Sci., Part A: Polym. Chem.* **2004**, *42*, 5523–5529. (b) Xu, X.; Huang, J. *J. Polym. Sci., Part A: Polym. Chem.* **2006**, *44*, 467–476.

(24) Hernández-Guerrero, M.; Davis, T. P.; Barner-Kowollik, C.; Stenzel, M. H. *Eur. Polym. J.* **2005**, *41*, 2264–2277.

(25) Hirschmann, R. P.; Kniseley, R. N.; Fassel, V. A. *Spectrochim. Acta* **1965**, *12*, 2125–2133.

(26) Broadening of PDI after heating to 200 °C was reported in PLLA-*b*-PHEMA case. See: Wolf, F. F.; Friedemann, N.; Frey, H. *Macromolecules* **2009**, *42*, 5622–5628.

(27) Perova, T. S.; Vij, J. K.; Xu, H. *Colloid Polym. Sci.* **1997**, *275*, 323–332.

(28) (a) Vincendon, M. *Makromol. Chem.* **1993**, *19*, 321–328. (b) Furer, V. L. *J. Appl. Spectrosc.* **1990**, *53*, 270–275.

(29) Houghton, R. P.; Mulvaney, A. W. *J. Organomet. Chem.* **1996**, *518*, 21–27.

(30) Meares, P. *Polymers: Structure and Bulk Properties*; Van Nostrand Reinhold Company Ltd.: London, 1965; Chapter 10.

(31) Pollet, E.; Delcourt, C.; Alexandre, M.; Dubois, P. *Eur. Polym. J.* **2006**, *42*, 1330–1341.

(32) (a) Almdal, K.; Koppi, K. A.; Bates, F. S.; Mortensen, K. *Macromolecules* **1992**, *25*, 1743–1751. (b) Hamley, I. W.; Koppi, K. A.; Rosedale, J. H.; Bates, F. S.; Almdal, K.; Mortensen, K. *Macromolecules* **1993**, *26*, 5959–5970. (c) Förster, S.; Khandpur, A. K.; Zhao, J.; Bates, F. S.; Hamley, I. W.; Ryan, A. J.; Bras, W. *Macromolecules* **1994**, *27*, 6922–6935. (d) Zhao, J.; Majumdar, B.; Schulz, M. F.; Bates, F. S.; Almdal, K.; Mortensen, K.; Hajduk, D. A.; Gruner, S. M. *Macromolecules* **1996**, *29*, 1204–1215.

(33) (a) Hashimoto, T.; Koizumi, S.; Hasegawa, H.; Izumitani, T.; Hyde, S. T. *Macromolecules* **1992**, *25*, 1433–1439. (b) Disko, M. M.; Liang, K. S.; Behal, S. K.; Roe, R. J.; Jeon, K. J. *Macromolecules* **1993**, *26*, 2983–2986. (c) Mani, S.; Weiss, R. A.; Cantino, M. E.; Khairallah, L. H.; Hahn, S. F.; Williams, C. E. *Eur. Polym. J.* **2000**, *36*, 215–219. (d) Ahn, J.-H.; Zin, W.-C. *Macromolecules* **2000**, *33*, 641–644. (e) Zhu, L.; Huang, P.; Chen, W. Y.; Weng, X.; Cheng, S. Z. D.; Ge, Q.; Quirk, R. P.; Senador, T.; Shaw, M. T.; Thomas, E. L.; Lotz, B.; Hsiao, B. S.; Yeh, F.; Liu, L. *Macromolecules* **2003**, *36*, 3180–3188. (f) Ruokolainen, J.; Mezzenga, R.; Fredrickson, G. H.; Kramer, E. J.; Hustad, P. D.; Coates, G. W. *Macromolecules* **2005**, *38*, 851–860. (g) Valkama, S.; Ruotsalainen, T.; Nykänen, A.; Laiho, A.; Kosonen, H.; ten Brinke, G.; Ikkala, O.; Ruokolainen, J. *Macromolecules* **2006**, *39*, 9327–9336. (h) Rubatat, L.; Li, C.; Dietsch, H.; Nykänen, A.; Ruokolainen, J.; Mezzenga, R. *Macromolecules* **2008**, *41*, 8130–8137. (i) Mortensen, K.; Vigild, M. E. *Macromolecules* **2009**, *42*, 1685–1690.

(34) (a) Fredrickson, G. H. *Macromolecules* **1991**, *24*, 3456–3458. (b) Laradji, M.; Shi, A.-C.; Noolandi, J.; Desai, R. C. *Macromolecules* **1997**, *30*, 3242–3255. (c) Hajduk, D. A.; Ho, R.-M.; Hillmyer, M. A.; Bates, F. S.; Almdal, K. *J. Phys. Chem. B* **1998**, *102*, 1356–1363. (d) Hamley, I. W.; Fairclough, J. P. A.; Ryan, A. J.; Mai, S.-M.; Booth, C. *Phys. Chem. Chem. Phys.* **1999**, *1*, 2097–2101. (e) Wang, C.-Y.; Lodge, T. P. *Macromolecules* **2002**, *35*, 6997–7006. (f) Lai, C.; Loo, Y.-L.; Register, R. A.; Adamson, D. H. *Macromolecules* **2005**, *38*, 7098–7104.

(35) Hameed, N.; Guo, Q.; Xu, Z.; Hanley, T. L.; Mai, Y.-W. *Soft Matter* **2010**, *6*, 6119–6129.

(36) Chow, C. D. *J. Polym. Sci., Polym. Chem. Ed.* **1975**, *13*, 309–313.